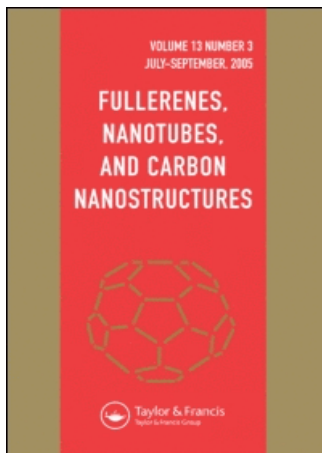


This article was downloaded by:[NEICON Consortium]
On: 1 August 2007
Access Details: [subscription number 762905488]
Publisher: Taylor & Francis
Informa Ltd Registered in England and Wales Registered Number: 1072954
Registered office: Mortimer House, 37-41 Mortimer Street, London W1T 3JH, UK



Fullerenes, Nanotubes and Carbon Nanostructures

Publication details, including instructions for authors and subscription information:
<http://www.informaworld.com/smpp/title~content=t713597253>

Why are Solutions of C₆₀-Piperazine Purple at pH 11?

Online Publication Date: 01 July 2007

To cite this Article: Xu, Hanying, Tian, Jun, Korobov, Mikhail V., Sohlberg, Karl and Smith, Allan (2007) 'Why are Solutions of C₆₀-Piperazine Purple at pH 11?', Fullerenes, Nanotubes and Carbon Nanostructures, 15:4, 267 - 277

To link to this article: DOI: 10.1080/15363830701421512

URL: <http://dx.doi.org/10.1080/15363830701421512>

PLEASE SCROLL DOWN FOR ARTICLE

Full terms and conditions of use: <http://www.informaworld.com/terms-and-conditions-of-access.pdf>

This article maybe used for research, teaching and private study purposes. Any substantial or systematic reproduction, re-distribution, re-selling, loan or sub-licensing, systematic supply or distribution in any form to anyone is expressly forbidden.

The publisher does not give any warranty express or implied or make any representation that the contents will be complete or accurate or up to date. The accuracy of any instructions, formulae and drug doses should be independently verified with primary sources. The publisher shall not be liable for any loss, actions, claims, proceedings, demand or costs or damages whatsoever or howsoever caused arising directly or indirectly in connection with or arising out of the use of this material.

© Taylor and Francis 2007

Fullerenes, Nanotubes, and Carbon Nanostructures, 15: 267–277, 2007

Copyright © Taylor & Francis Group, LLC

ISSN 1536-383X print/1536-4046 online

DOI: 10.1080/15363830701421512



Why are Solutions of C₆₀-Piperazine Purple at pH 11?

Hanying Xu

Department of Physical Sciences, Kingsborough Community College,
Brooklyn, New York, USA

Jun Tian

Chemistry Department, Shanghai University, Shanghai, China

Mikhail V. Korobov

Chemistry Department, Moscow State University, Moscow, Russia

Karl Sohlberg, and Allan Smith

Department of Chemistry, Drexel University, Philadelphia,
Pennsylvania

Abstract: The C₆₀-piperazine mono adduct was synthesized by the reaction of C₆₀ and piperazine. The saturated C₆₀-piperazine aqueous solution was colorless when pH is 8 or below. A purple color was developed when pH is around 9 and the pink color is most intense at pH 11. The color of the C₆₀-piperazine solution fades out when pH is approaching 12 from 11, and the solution remains colorless when pH is 13 or higher. The UV-Vis spectra of the C₆₀-piperazine solution were recorded at pH 4, 11 and 14. The mono-protonated C₆₀-piperazine was identified to be responsible for the purple color observed. The computational investigation of the un-protonated, mono-protonated and di-protonated C₆₀-piperazine was conducted at the PM3 and ZINDO(s) levels of theory. Vibronic coupling of the Jahn-Teller active vibrational mode to the electronic transition was applied to re-generate the weak absorption between 550–600 nm in the UV-Vis spectrum of the mono-protonated C₆₀-piperazine.

Keywords: C₆₀-piperazine mono adduct, vibronic coupling, Jahn-Teller active vibrational mode, PM3, ZINDO(s)

Received 6 September 2006, Accepted 21 October 2006

Address correspondence to Dr. Hanying Xu, Department of Physical Sciences, Kingsborough Community College, 2001 Oriental Boulevard, Brooklyn, NY 11235, USA. E-mail: hy_xu@yahoo.com

INTRODUCTION

There is currently a great deal of interest in derivatized fullerenes because of the attractiveness of combining chemically useful functionality with their unique chemical, physical and electronic properties. An example is C_{60} -piperazine adducts, which have been investigated both experimentally (1) and theoretically (2). The C_{60} -piperazine molecule itself is a tertiary di-amine, which is a weak organic base and may exist as the neutral species ($C_{60}P$), the mono-protonated species ($C_{60}PH^+$) and the di-protonated $C_{60}PH_2^+$ species (Figure 1). The experimental research on the UV-Vis spectra of aqueous C_{60} -piperazine solutions has produced a curious result: C_{60} -piperazine solution is colorless when the pH is below 6 or if the pH is around 14, but has a purple color at pH 11.

Here, we report experimental and theoretical studies of C_{60} -piperazine and its mono- and di-protonated analogues (see Figure 1) aiming to elucidate the origin of these color changes. First, a thermodynamic model of the composition of an aqueous solution of C_{60} -piperazine was constructed that predicts the composition of the solution as a function of pH (Figure 2). Next, UV-Vis spectra of the C_{60} -piperazine solution were recorded at pH 4, 11 and 14 in order to verify the model and determine the equilibrium constants therein.

The results show that the dominant species is di-protonated C_{60} -piperazine at pH 4 in the C_{60} -piperazine solution, while the neutral C_{60} -piperazine dominates at pH 14. The mono-protonated C_{60} -piperazine adduct is the major component at pH 11, suggesting that this species is responsible for the purple color. Finally C_{60} -piperazine, the mono-protonated C_{60} -piperazine adduct and the di-protonated C_{60} -piperazine adduct were investigated using ab-initio quantum chemical methods. Calculations of the spectra of each species confirms that the mono-protonated C_{60} -piperazine has a weak absorption in the green, caused by Jahn-Teller distortion of the C_{60} . This absorption is responsible for the purple color of the pH 11 solutions.

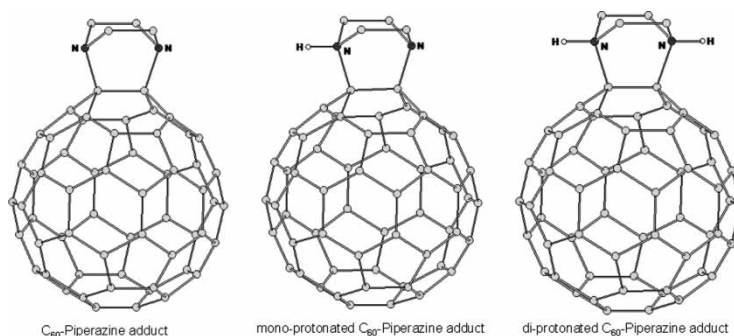


Figure 1. Structures of the neutral C_{60} -piperazine adduct (C_{2v} symmetry), the mono-protonated C_{60} -piperazine (C_s symmetry) and the di-protonated C_{60} -piperazine (C_{2v} symmetry).

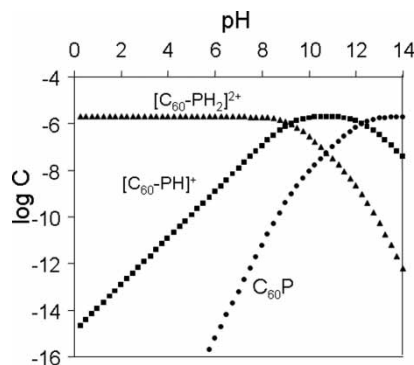


Figure 2. The components of the C₆₀-piperazine solution as a function of pH values. (C₆₀P: the neutral C₆₀-piperazine adduct; [C₆₀PH]⁺: the mono-protonated C₆₀-piperazine adduct; [C₆₀PH₂]²⁺: the di-protonated C₆₀-piperazine adduct).

EXPERIMENTAL METHODS

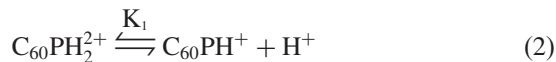
C₆₀-piperazine mono-adduct was synthesized for this investigation by the reactions of C₆₀ (MER Corporation, Tucson, AZ) and piperazine (Sigma-Aldrich) in toluene (Fisher Scientific) with 1:1 molar ratio of C₆₀ and piperazine (1). The chemicals were used without further purification. The reactions were conducted in a 50°C water bath for 7 days. The C₆₀-piperazine mono-adduct was purified by column chromatography using 100:1 (v/v) methylene chloride: methanol as the mobile phase and the 30-inch long glass column with the internal diameter of 1 inch, and characterized by ¹H NMR (Bruker 250 MHz, Drexel University) and mass spectrometry.

The saturated C₆₀-piperazine aqueous solution (2.7 mg/L) is clear and colorless when pH is below 8. When pH is approaching 9, a pink-like color is gradually developed and is most intense around pH 11. The color of the saturated C₆₀-piperazine solution fades away when the pH is over 12 and the saturated solution remains colorless when pH is 13 or higher. Combining the basic property of the C₆₀-piperazine molecule and the observed color changes of the C₆₀-piperazine solution, it can be postulated that the C₆₀PH₂²⁺, C₆₀PH⁺ and C₆₀P are the dominating species when pH is below 9, pH is between 9 and 12, and pH is 12 and higher, respectively.

A thermodynamic model of composition as the function of pH of C₆₀-piperazine solutions was carried out to support the postulation. The C₆₀-piperazine is a tertiary di-amine, which exists as the neutral species (C₆₀P) and can be protonated giving mono-protonated species (C₆₀PH⁺) and/or di-protonated C₆₀PH₂²⁺ compound depending on the pH values of the solution. Therefore, equation (1) can be established (ref. (1)):

$$[\text{C}_{60}\text{P}]_{\text{total}} = [\text{C}_{60}\text{P}] + [\text{C}_{60}\text{PH}^+] + [\text{C}_{60}\text{PH}_2^{2+}] \quad (1)$$

The equilibria among the neutral $C_{60}P$, $C_{60}PH^+$ and $C_{60}PH_2^{2+}$ are given by equations (2) and (3):



The equilibrium constants K_1 and K_2 are defined as follows:

$$K_1 = \frac{[C_{60}PH^+][H^+]}{[C_{60}PH_2^{2+}]} \quad (4)$$

$$K_2 = \frac{[C_{60}P][H^+]}{[C_{60}PH^+]} \quad (5)$$

Equations (4) and (5) are applied to equation (1) to give equation (6):

$$[C_{60}P]_{\text{total}} = \frac{K_2[C_{60}PH^+]}{[H^+]} + [C_{60}PH^+] = \frac{[C_{60}PH^+][H^+]}{[K^+]} \quad (6)$$

Then, equation (6) can be rearranged to equation (7):

$$\frac{[C_{60}PH^+]}{[C_{60}P]_{\text{total}}} = \frac{1}{1 + K_2/[H^+] + [H^+]/K_1} \quad (7)$$

The total concentration of $C_{60}P$ is known and the $[H^+]$ can be measured with a pH meter. There are 3 variables in equation (7), $[C_{60}PH^+]$, K_1 and K_2 . The C_{60} -piperazine solutions have visible colors when the pH values are between 9 and 12. Therefore, Beer's Law will be applied to give $[C_{60}PH^+]$ (1). Then, 15 C_{60} -piperazine aqueous solutions were made with the pH values between 9 and 12 and the UV-Vis spectra of these 15 solutions were recorded to determine the λ_{max} in the visible region (400–760 nm). It was found that the λ_{max} is 554 nm (1). Accordingly, equation (8) can be obtained:

$$A(554 \text{ nm}) = \varepsilon * b * [C_{60}PH^+] \quad (8)$$

Combining equations (7) and (8), equation 9 is derived:

$$\frac{A(554 \text{ nm})}{[C_{60}P]_{\text{total}}} = \frac{\varepsilon * b}{1 + K_2/[H^+] + [H^+]/K_1} \quad (9)$$

In equation (9), $[C_{60}P]_{\text{total}}$ is known, $A(554 \text{ nm})$ is the measured absorbance, and K_1 , K_2 and $\varepsilon * b$ are unknown constants. Once the series of $A(554 \text{ nm})$ along with the corresponding $[H^+]$ were obtained, Origin 6.1 (Microcal Corp., MA) was applied to fit these data to obtain the 3 unknown constants (i.e., K_1 , K_2 and $\varepsilon * b$) in equation (9). The K_1 and K_2 were determined ($T = 298 \text{ K}$) as follows (1):

$$K_1 = 1.2 \times 10^{-9}, \quad K_2 = 6.6 \times 10^{-13}$$

Using equations (4), (5) and (7), [C₆₀P], [C₆₀PH⁺] and [C₆₀PH₂²⁺] were determined at different pH values. The corresponding plot of the compositions vs. pH values is shown in Figure 2.

It is clear that the di-protonated C₆₀PH₂²⁺ is the major species at pH 8 or lower, the mono-protonated C₆₀PH⁺ dominates around pH 11 and the neutral C₆₀-piperazine (un-protonated) is the dominant one at pH 13 or higher. This result is consistent with the postulation stated here. The experimental oscillator strengths were converted from the corresponding molar extinction coefficients by equation (10) (see ref. (3)). The integral in equation (10) was evaluated numerically (trapezoid rule).

$$\text{Oscillator strength } f = 4.33 * 10^{-9} * \int \varepsilon(\lambda) d\lambda^{-1} \quad (10)$$

where $\varepsilon(\lambda)$ is the extinction coefficient.

COMPUTATIONAL METHODS

The geometrical structures of C₆₀-piperazine, mono-protonated and di-protonated C₆₀-piperazine were first optimized at the MM+ (4) level of theory to generate reasonable starting structures for further quantum mechanical calculations. C₆₀-piperazine, mono-protonated and di-protonated C₆₀-piperazine were then fully optimized based on the semiempirical PM3 (5) Hamiltonian. Vibrational spectra of these three species were calculated based on the fully optimized structures at the PM3 level. Single point calculations, (based on the ZINDO(s) (6) Hamiltonian and a truncated configuration interaction (CI) basis of single excitations) were then carried out to generate the corresponding UV-Vis spectra. The 35 highest occupied MOs and 35 lowest unoccupied MOs, 40 highest occupied MOs and 40 lowest unoccupied MOs and 30 highest occupied MOs and 30 lowest unoccupied MOs were included in the ZINDO(s) calculations of C₆₀-piperazine, mono-protonated and di-protonated C₆₀-piperazine, respectively. These CI bases were selected based on convergence tests on the related species 2,3-dihydro-1,4-ethano-quinoxaline (Figure 3) and on natural energy gaps in the MO eigenvalue spectra. All the calculations were carried out using HyperChem software (7).

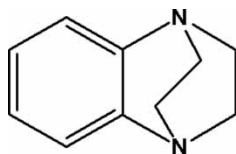


Figure 3. The structure of 2,3-dihydro-1,4-ethano-quinoxaline.

Because of the structural similarity between 2,3-dihydro-1,4-ethano-quinoxaline (Figure 3) and C₆₀-piperazine (Figure 1), the UV-Vis spectrum of 2,3-dihydro-1,4-ethano-quinoxaline was computed with the same theoretical methodology and compared to its experimental data in order to test the reliability of the method used for this project. 2,3-dihydro-1,4-ethano-quinoxaline (See Figure 3) was purchased from ChemDiv, Inc., San Diego, CA. UV-Vis spectra were obtained using an HP 8431 Diode array UV-Vis spectrophotometer.

An interval of 5 nm has been used to calculate the oscillator strengths in order to match the experimental resolution. A moving average (7 points, 30 nm wide) has been applied to each theoretical spectrum to mimic the experimental broadening.

RESULTS AND DISCUSSION

The Reliability of the Computational Method Applied in this Project

To establish the reliability of the computational methods applied in this project, the methods used were applied to the related species 2,3-dihydro-1,4-ethano-quinoxaline. Theoretical and experimental UV adsorption maxima for 2,3-dihydro-1,4-ethano-quinoxaline are shown in Table 1. It can be seen that the calculated λ_{\max} values are good in agreement with the experimental data as are the *relative* oscillator strengths. These results benchmark the accuracy of the theoretical and computational methods used. Based on the structural similarity of 2,3-Dihydro-1,4-ethano-quinoxaline to C₆₀-piperazine, we expect similar accuracy for the C₆₀-piperazine spectra reported here.

To further support the choice of theoretical methods, the computed adsorption wavelengths and oscillator strengths of C₆₀-piperazine between 400 and 600 nm are tabulated in Table 2, where they are compared to published results (2). Again the agreement is found to be quite satisfactory. Therefore, the computational method used in this paper is deemed suitable for reproducing the UV-Vis spectra for C₆₀-piperazine and its derivatives.

Table 1. Comparison of the experimental data and the computational results of 2,3-Dihydro-1,4-ethano-quinoxaline

	Wavelength λ_{\max} (nm)	Oscillator strength f	Relative oscillator strength f
Expt	206	6.09	1
	256	0.25	0.041
	262	0.065	0.011
Theo.	207	1.61	1
	248	0.067	0.042
	278	0.030	0.019

Table 2. Computational results from wavelengths above 400 nm for C₆₀-piperazine and comparison with published results (2)

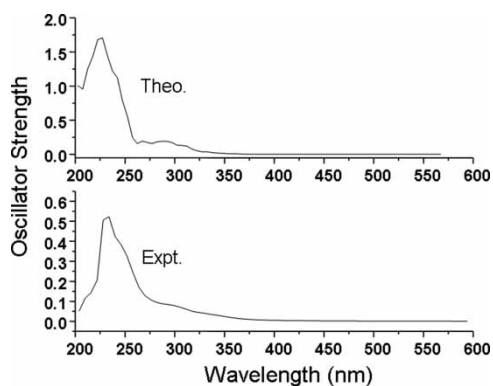
Present work		Theoretical results from Ref. (2)	
Wavelength (nm)	Oscillator strength	Wavelength (nm)	Oscillator strength
567.3	0.0059	599.3	0.0071
500.1	0.0014	512.6	0.0016
482.3	0.0033	500.7	0.0025
444.1	0.0014	450.5	0.0014
438.5	0.0024	435.0	0.0012
425.2	0.0125	432.9	0.0166

C₆₀-Piperazine Adduct

The measured UV-Vis spectrum of C₆₀-piperazine is depicted in Figure 4 and compared with the theoretical results. The λ_{max} of the theoretically generated spectrum is around 225 nm. This curve levels off above 400 nm, which is in agreement with the fact that the C₆₀-piperazine solution is colorless at pH 14 where the unprotonated species dominates. The UV-Vis spectrum obtained experimentally is very similar, having λ_{max} of about 230 nm and no peak above 400 nm.

Mono-Protonated C₆₀-Piperazine

Figure 5 shows the experimental (bottom) and theoretical (top) UV-Vis spectra of the mono-protonated C₆₀-piperazine. The two are in accord except that the missing little “bump” centered at 554 nm in the measured

**Figure 4.** Comparison of the experimental UV-VIS spectrum (bottom) with the theoretical one (top) for C₆₀-piperazine.

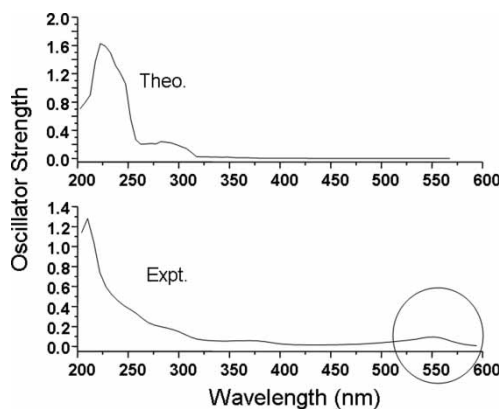


Figure 5. Comparison of the experimental curve (bottom) with the theoretical ones (top) for the mono-protonated C_{60} -piperazine, $[C_{60}PH]^+$.

spectrum is not reproduced theoretically. Theoretically the C_{60} -piperazine solution at pH 11 should therefore be colorless. Experimentally it gives an intense purple color at pH 11.

To understand the source of the long-wavelength adsorption of mono-protonated C_{60} -piperazine, we first consider unmodified C_{60} itself (8–12). C_{60} has I_h symmetry. T_{1g} , T_{2g} and G_g are the irreducible representations of the lowest excited states (10). The lowest lying transitions (HOMO \rightarrow LUMO, LUMO + 1, LUMO + 2) are therefore inversion-symmetry forbidden (8–12). It has been proposed that broad weak bands in the visible range of the experimental UV-Vis spectra of C_{60} (11) correspond to these electronically forbidden transitions, and that vibronic coupling breaks the inversion-symmetry selection rule (8–12). For the C_{60} molecule, vibrations with suitable symmetries (Herzberg–Teller and/or Jahn–Teller active modes) may bring intensity borrowing to allow these forbidden transitions (8–12).

By analogy to C_{60} , vibronic coupling is proposed here to explain the origin of the absorption in the visible range in the UV-Vis spectrum of the mono-protonated C_{60} -piperazine solution. To test this hypothesis, the vibrational spectra of both C_{60} and the mono-protonated C_{60} -piperazine were calculated at the PM3 level of theory.

At room temperature, the most populated Jahn–Teller active normal mode of C_{60} was found to have h_g symmetry (h_g symmetry vibrational mode is Jahn–Teller active for C_{60} (9–11) and a frequency of 266.5 cm^{-1}). This h_g vibrational mode with the frequency of 266.5 cm^{-1} induces intensity borrowing through vibronic coupling. One of the most populated normal modes of the mono-protonated C_{60} -piperazine has a' symmetry and a frequency of 217.2 cm^{-1} . In this normal mode (a' , 217.2 cm^{-1}), the C_{60} moiety of the mono-protonated C_{60} -piperazine molecule follows the same vibrational pattern as the J-T active mode (h_g , 266.5 cm^{-1}) in C_{60} .

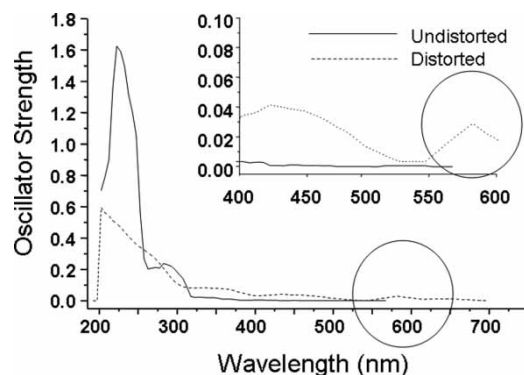


Figure 6. Comparison of the theoretically reproduced UV-Vis curves of the mono-protonated C₆₀-piperazine (in solid line) with the distorted mono-protonated C₆₀-piperazine (in dashed line) along a specific normal mode (*a'* symmetry, 217.2 cm⁻¹). The inset is the same plot enlarged between 410 and 600 nm.

To see if the (*a'*, 217.2 cm⁻¹) mode in mono-protonated C₆₀-piperazine can give rise to UV-Vis absorption through vibronic coupling, the geometry of the mono-protonated C₆₀-piperazine was distorted along the normal mode (*a'*, 217.2 cm⁻¹) and the electronic spectrum of the distorted mono-protonated C₆₀-piperazine computed using ZINDO(s). A comparison of UV-Vis spectra for the equilibrium structure of mono-protonated C₆₀-piperazine (solid line) and the distorted mono-protonated C₆₀-piperazine (dashed line) is depicted in Figure 6. The oscillator strengths between 410 nm and 600 nm of the distorted mono-protonated C₆₀-piperazine are significantly larger in magnitude than the corresponding ones for the mono-protonated C₆₀-piperazine (Figure 6).

For example, the oscillator strength at 432.5 nm is about 50 times stronger in the UV-Vis spectrum of the distorted mono-protonated C₆₀-piperazine than that of the equilibrium structure of mono-protonated C₆₀-piperazine (Figure 6). In addition, this introduction of vibronic coupling does produce a broad weak peak theoretically centered at 585 nm in the predicted UV-Vis spectrum. λ_{max} for this peak differs by only 6% from the experimental result, very good agreement given the simplicity of theoretical model (the inset in Figure 6). Therefore, we conclude that vibronic coupling is a likely explanation for the missing peak in the visible range in the UV-Vis spectrum of the mono-protonated C₆₀-piperazine.

Di-Protonated C₆₀-Piperazine

The experimental (bottom) and the theoretical (top) UV-Vis spectra of the di-protonated C₆₀-piperazine are illustrated in Figure 7. There are three

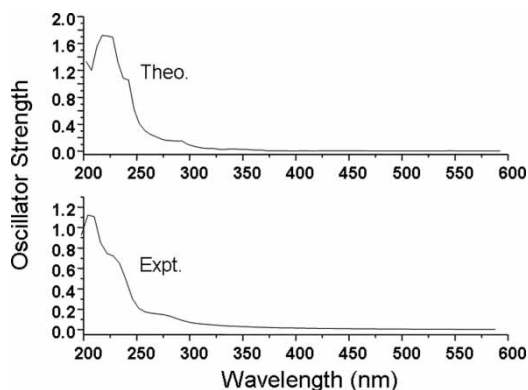


Figure 7. Comparison of the experimental UV-Vis spectrum (bottom) with the theoretical one (top) for the di-protonated C_{60} -piperazine, $[C_{60}PH_2]^{2+}$.

major absorptions (210 nm, 225 nm and 275 nm) in the experimentally recorded UV-Vis spectrum of the di-protonated C_{60} -piperazine. In the theoretically reproduced UV-Vis spectrum, the corresponding peaks are at 225 nm, 240 nm and 285 nm, respectively. The theoretical curve is again qualitatively consistent with the experimental data and both support the observation of colorless C_{60} -piperazine solution at low pH.

CONCLUSIONS

The electronic spectra of C_{60} -piperazine, mono-protonated C_{60} -piperazine and di-protonated C_{60} -piperazine were calculated theoretically and compared to the corresponding experimental curves. ZINDO(s) spectra of C_{60} -piperazine and di-protonated C_{60} -piperazine are qualitatively consistent with the experimental results. A broad weak peak centered at 554 nm in the experimentally obtained UV-Vis spectrum of the mono-protonated C_{60} -piperazine was successfully reproduced theoretically by introducing vibronic coupling.

The theoretically reproduced broad peak with low intensity in the UV-Vis spectrum of the mono-protonated C_{60} -piperazine is centered at 585 nm, a relative error of about 6% compared to the experimental data. This result supports the hypothesis that mono-protonated C_{60} -piperazine gives a colored solution because of a weak adsorption in the 550–600 nm region of the visible range due to vibronic coupling of the (a' , 217.2 cm^{-1}) JT-active vibrational mode to the electronic transition. Vibration along this mode distorts mono-protonated C_{60} -piperazine in an analogous way to a known J-T active mode in un-derivatized C_{60} .

ACKNOWLEDGMENT

We are grateful to Sister Rose Mulligan for her friendly help. H. Xu would like to thank Ari Silver for assistance adapting software. MVK is grateful to RFBR (grant 06-03-32446) for the financial support.

REFERENCES

1. (a) Tian, J. (2003) Comparative solubility study of C₆₀ and C₆₀-Piperazine and applications on quartz crystal microbalance/heat conduction calorimeter, Ph.D. Thesis, Drexel University; (b) Tian, J., Scheesley, D., Smith, A.L., Stukalin, E., Avramenko, N., and Korobov, M. (2001) *Recent Advances in the Chemistry and Physics of Fullerenes and Related Materials*; Kadish, K. (ed.); Proceedings-Electrochemical Society, ECS Publication: Pennington, NJ, Vol. 11, 381–393.
2. Chen, Z., Teng, Q., Wu, S., Pan, Y., Zhao, X., Tang, A., and Feng, J. (1998) Quantum chemical studies on the structures and spectra for the addition product C₆₄N₂H₈. *Chem. Res. Appl.*, 10 (1): 38–42.
3. Harris, D.C. and Bertolucci, M.D. (1989) *Symmetry and Spectroscopy: An Introduction to Vibrational and Electronic Spectroscopy*; Dover Publications, Inc.: New York.
4. Allinger, N.L. (1977) Conformational analysis. 130. MM2. A hydrocarbon force field utilizing V1 and V2 torsional terms. *J. Am. Chem. Soc.*, 99: 8127–8134.
5. (a) Stewart, J.J.P. (1989) Optimization of parameters for semiempirical methods I. Method. *J. Comput. Chem.*, 10: 209–220; (b) Stewart, J.J.P. (1989) Optimization of parameters for semiempirical methods II. Applications. *J. Comput. Chem.*, 10: 221–264.
6. Anderson, W.P., Edwards, W.D., and Zerner, M.C. (1986) Calculated spectra of hydrated ions of the first transition-metal series. *Inorg. Chem.*, 25: 2728–2732.
7. HyperChem Version 6.0 for Windows. (2000) HyperCube, Inc.
8. Bendale, R.D., Baker, J.D., and Zerner, M. (1991) Calculations on the electronic structure and spectroscopy of C₆₀ and C₇₀ cage structures. *Int. J. Quantum Chem.*, 25: 557–568.
9. Negri, F., Orlandi, G., and Zerbetto, F. (1996) Assignments in the 600 nm region of C₆₀: The origins of the T_{1g} and G_g transitions. *J. Phys. Chem.*, 100: 10849–10853.
10. Negri, F., Orlandi, G., and Zerbetto, F. (1992) Interpretation of the vibrational structure of the emission and absorption spectra of C₆₀. *J. Chem. Phys.*, 97: 6496–6503.
11. Leach, S. (1994) Electronic spectroscopy and photophysics of fullerenes. *NATO ASI Series, Series C.*, 443: 117–140.
12. Whetten, R.L., Alvarez, M.M., Anz, S.J., Schriver, K.E., Beck, R.D., Diederich, F.N., Rubin, Y., Ettl, R., Foote, C.S., Darmanyan, A.P., and Arbogast, J.W. (1991) Spectroscopic and photophysical properties of the soluble C_n molecules, n = 60, 70, 76/78, 84. *Materials Research Society Symposia Proceedings*, 206: 639–650.